The Trapping of the OH Radical by Coenzyme Q. A Theoretical and Experimental Study

J. Espinosa-García*,† and C. Gutiérrez-Merino‡

Dept. de Química Física, and Dept. de Bioquímica y Biología Molecular y Genética, Facultad de Ciencias, Universidad de Extremadura, 06071 Badajoz (Spain)

Received: July 4, 2003; In Final Form: August 29, 2003

Several pathways for the attack of the hydroxyl radical on coenzyme Q, as a prototypical chemical reaction involved in biological antioxidant actions, were theoretically analyzed by hybrid density functional theory computations, at the BHandHLYP/6-31G level. We found that the most favorable pathways are the hydrogen abstraction reaction from the phenolic hydrogen on the reduced form (ubiquinol), and the electrophilic OH addition on the oxidized form (ubiquinone). The reaction paths for the two mechanisms were traced independently. Following the direct dynamics method, the respective thermal rate constants were calculated using variational transition-state theory with multidimensional small-curvature tunneling. The experimental rate constants for the reaction of ubiquinol and ubiquinone with hydroxyl radicals produced via the Fenton's reaction in phosphate-buffered water solution at pH 7 were also measured. We found, first, that the reactivity in gas-phase (theoretical approach) is dominated by the OH addition mechanism on ubiquinone, and second, that a good agreement exists between the ratio of the rate constants determined from theoretical and experimental approaches for the reaction of oxidized and reduced forms of coenzyme Q with hydroxyl radicals. It is a very fast reaction, practically diffusion-controlled, with an inverse dependence of the thermal rate constants on temperature and therefore, a negative activation energy, both theoretically and experimentally. The influence of the tunneling factor was negligible. The analysis of the enthalpy and entropy contributions to the Gibbs free energy profile allowed us to understand the negative value of the activation energy.

1. Introduction

Free radicals are ubiquitous compounds in nature. They play an important role in atmospheric and combustion chemistry,[1,2] radiative and nonradiative processes,[3−5] and in the chemistry of life.[6,7] They have also been implicated in inflammation, ischaemia, and a wide variety of degenerative diseases[8,9] and in processes underlying biological aging.[10,11]

Chain-breaking reactions are known to be efficient protection against free radical reaction damage. Natural radical-trapping antioxidants such as coenzyme Q (CoQ) and α-tocopherol (vitamin E), which partitions in the lipid bilayer, can avoid or at least significantly reduce free radical reaction damage in a lipid environment[12−15] (Scheme 1). As a result they afford efficient antioxidant protection to biological membranes[13,16,17] and to human low-density lipoproteins (LDL).[18−22]

Note that the isoprenoid units can vary from 6 in some yeasts to 10 in humans,[23] and that ubiquinol (UQH_2) is the reduced form of ubiquinone (UQ), mitoquinone, or coenzyme Q, by a two-electron process[24] (Scheme 2).

Although strictly speaking the coenzyme Q denomination is reserved for the oxidized ubiquinone form, to make the discussion clearer we will use the denominations ubiquinone (UQ) and ubiquinol (UQH_2) for the oxidized and reduced forms, respectively, retaining the name coenzyme Q as a general description of the redox system. In living cells coenzyme Q functions as an obligatory chemical intermediate electron carrier in the electron transport chains of mitochondria[24,25] and plasma membranes,[26] and it has been shown that NADH and ascorbic acid play major roles as electron donors for the reduction of oxidized coenzyme Q in mammalian cells.[26−28] In mammalian cells, most of the dehydroascorbic acid produced upon the oxidation of ascorbic acid is reduced by redox coupling to glutathione.[29] Because the intracellular concentration of reduced gluthatione is a good indicator of the intracellular redox state,[30] it follows that within the living cells the chemical equilibrium between oxidized and reduced coenzyme Q is altered under oxidative stress conditions (such as those produced in ischaemia

SCHEME 1

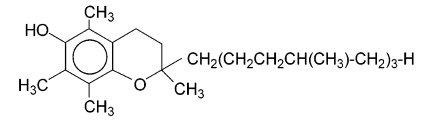

α-tocopherol

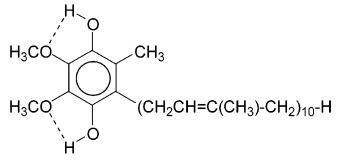

Ubiquinol-10

SCHEME 2

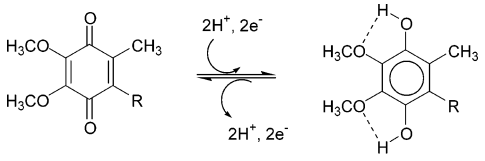

UQ (Ubiquinone) UQH_2 (Ubiquinol)

* Corresponding author. E-mail: joaquin@unex.es. To my father. In Memoriam (September 22, 2003).
† Dept. de Química Física.
‡ Dept. de Bioquímica y Biología Molecular y Genética.

10.1021/jp035927a CCC: $25.00
Published on Web 10/21/2003

or inflammation) that lead to depletion of intracellular reduced gluthatione.[30,31] Under these conditions a large increase of oxygen radical species, hydroxyl radicals among them, is observed within the cells.[9]

The peroxidation of lipids (LH) is a free radical chain reaction that yields peroxyl radicals (LOO.)[32,33]

$$LH \xrightarrow{O_2} LOO^{\bullet}$$

It is generally accepted that most free radical trapping antioxidants (AH) capture these radicals by a hydrogen abstraction reaction[33]

$$LOO^{\bullet} + AH \rightarrow LOOH + A^{\bullet}$$

where the resultant antioxidant radical $A^{\bullet}$ is expected to be unreactive, to form the corresponding dimer, or to react with another free radical to yield nonradical products.

Considerable experimental work has been devoted to the study of the activity of free radical chain-breaking antioxidants on biological systems.[34−43] These studies concluded that the relative antioxidant activities of QH_2 vs α-TOH are QH_2 > α-TOH in LDL; QH_2 < α-TOH in homogeneous solution; and $QH_2 \approx$ α-TOH in aqueous lipid dispersions,[35] and that the oxidized form of QH_2, i.e., ubiquinone, has little or no antioxidant activity.[44−46] The reaction between the CoQ and the hydroxyl radical has not been experimentally studied: will this free radical follow the same mechanism of hydrogen abstraction reaction as the peroxyl radicals? Will the oxidized form (ubiquinone) show little or no activity in the presence of the reactive and, therefore poorly selective, hydroxyl radical?

The extensive experimental literature on the reactivity of antioxidants contrasts with the scarce theoretical studies done on this subject despite its relevance, probably due to the difficulties in describing the electronic structure of these relatively large systems for this aim. Focusing on the coenzyme Q system, these studies have been limited to the stationary point geometries using molecular orbital methods. Thus, Heer et al.[41] applied hybrid density functional theory (DFT) at the B3LYP/6-31G(d,p) level to calculate the phenolic-hydrogen bond dissociation enthalpy of ubiquinol-0, 78.5 ± 1.5 kcal mol^{-1}, comparable with α-tocopherol BDE(O−H) of 77.3 kcal mol^{-1}.[47] Later, Ingold et al.[43] using the same hybrid DFT level, carried out transition state calculations for hydrogen abstraction reactions by methoxyl radicals from intramolecularly hydrogen-bonded and non-hydrogen-bonded 2-methoxyphenol (a very simple model of ubiquinol-0). They concluded that the hydrogen atom abstraction is surprisingly easy from intramolecularly hydrogen bonded methoxyphenols. Finally, Türker[48] performed a theoretical study on coenzyme Q_{10} (ubiquinone and ubiquinol) using the semiempirical orbital molecular method Austin model 1 (AM1).[49]

In this paper, we focus on the reaction of the hydroxyl radical ($^{\bullet}$OH), one of the most damaging free radicals that can arise in living organisms,[7] with coenzyme Q, which is present in all membranes of mammalian cells.[50] It is necessary to note that this relevant bioreaction has been neither theoretically nor experimentally reported to date, and its mechanism and kinetics, to the best of our knowledge, have not been analyzed. This reaction is expected to be very fast, because previous experimental studies[51] have shown that the second-order rate constant for the reaction of benzohydroquinone with $^{\bullet}$OH is greater than 10^9 M^{-1} s^{-1}.

The major aims of this paper are: first, to propose a mechanism to account for the attack of the hydroxyl free radical on CoQ, i.e., to analyze theoretically the possible reaction pathways, considering separately the oxidized and reduced forms of CoQ; second, to obtain theoretical kinetic information for the more favorable pathways; and third, to contrast theoretical kinetic predictions (which simulate a diluted gas-phase) with the experimentally determined rate contants in water solution at pH 7. In section II we describe the theoretical methods and computational details, and the experimental methods used in this work. Results and discussion are given in section III and, finally, conclusions are presented in section IV.

2. Methods

2.1. Theory, Methods, and Computational Details. Geometries, energies, and first and second energy derivatives of all stationary points were calculated by hybrid density functional theory (DFT) using the Gaussian 98[52] system of programs. Exchange and correlation were treated by the BHandHLYP method, which is based on Becke's half-and-half method[53] and the gradient-corrected correlation functional of Lee, Yang, and Parr,[54] using the 6-31G basis set. In short, the level used is named BHandHLYP/6-31G. It has been found that this hybrid DFT method gives more accurate barrier heights than other hybrid DFT methods, such as B3LYP and B3P86.[55−58] It has been pointed in the literature[59] that these methods present small spin contamination, with $\langle S^2 \rangle$ values calculated very close to the expectation values, i.e., 0.75. Note, however, that spin contamination in DFT calculations is not well defined theoretically and should be handled with caution,[60] although it can be expected that the problems for energy calculations associated with spin contamination are less severe in DFT than in ab initio theory.

Due to the large size of our molecular system and the great number of calculations (energies, gradients, and Hessians) along the reaction paths, the real biological reaction was modeled. First, Foti et al.[36] found that the hydrogen abstraction reaction from ubiquinol by phenoxyl radicals was independent of the number of isoprenoid units in the "tail", i.e., practically the same rate constants were found from 0 (ubiquinol-0) to 10 (ubiquinol-10) isoprenoid units. Based on these conclusions, the isoprenoid units in natural CoQ_{10} (see Scheme 1) were changed to a methyl group in this work. Second, while the theoretical study was performed in the gas-phase, given the nonpolar character of the natural environment (lipid bilayer), one can reasonably assume that the conclusions will be roughly the same in both environments. Note that, taking as reference the upper oxygen, the carbon atom positions will be labeled ipso, ortho, meta, and para for a clearer discussion in the following sections.

The kinetics study for the reaction of CoQ with OH was carried out using the direct dynamics approach.[61,62] This approach describes a chemical reaction by using electronic structure calculations of the energy and energy derivatives (gradients and Hessians) without the intermediary of an analytical potential energy surface or force field. In this approach, electronic structure calculations are required only in the region of configuration space lying along the reaction path and the reaction valley formed by the motion orthogonal to it. This method to construct the potential energy surface has already been used by our group to study smaller systems, in hydrogen abstraction[63−70] and addition reactions,[71] with excellent results.

Depending on whether the OH attack involved a barrier or not, two approaches were employed to calculate the initial information about the potential energy surface, which is needed to perform the kinetic study. (i) In the case that the reaction proceeds via a saddle point, i.e., a barrier height is involved,

we constructed the "intrinsic reaction coordinate" (IRC) or "minimum energy path" (MEP) at this level, with a gradient step size of 0.05 bohr amu$^{1/2}$, starting from the saddle point geometry and going downhill to both the asymptotic reactant and product channels in mass-weighted Cartesian coordinates. Along this MEP the reaction coordinate, *s*, is defined as the signed distance from the saddle point, with $s > 0$ referring to the product side. In the rest of the work the units of *s* are bohr, and the reduced mass to scale the coordinates is set to 1 amu. This has no effect on the calculated observables, but it does affect the magnitude of *s* in plots used for interpretative purposes. In this process one must be careful that electronic structure algorithms do not reorient the molecule. The reaction path was calculated from −0.5 bohr on the reactants side to +0.5 bohr on the product side. At each two points along the reaction path, the harmonic vibrational frequencies and reaction-path curvature components were computed. Along this MEP a generalized normal-mode analysis was performed, projecting out frequencies at each point along the path.[72] With this information we calculated the ground-state vibrationally adiabatic potential curve

$$V_a^G(s) = V_{MEP}(s) + \epsilon_{int}^G(s) \quad (1)$$

where $V_{MEP}(s)$ is the classical potential energy along the MEP with its zero energy at the reactants ($s = -\infty$) and $\epsilon_{int}^G(s)$ is the zero-point energy at *s* from the generalized normal-mode vibrations orthogonal to the reaction coordinate.

(ii) In the case that the reaction proceeds without saddle point, i.e., a barrierless reaction, we used the "distinguished coordinate path" (DCP approach),[73] where the most significant varying geometrical parameter, R_{C-O}, is fixed at different values and the other degrees of freedom are allowed to relax. In this case, the C−O distance ranges from 3.0 to 1.5 Å, i.e., practically from reactants to adducts. This DCP approach presents two main problems: molecular reorientation and incorrect projected normal-mode motions orthogonal to the path. To ensure that the orientation of the molecular system is consistent along the path, we used the algorithm proposed by Chen.[74] With respect to the second problem, while at each DCP point a generalized normal-mode analysis was performed, since the true MEP was not calculated, it must be borne in mind that projecting out the frequencies using the local gradient obtained from the DCP optimization may lead to incorrect results.[73] To obtain reliable eigenvectors and generalized frequencies along the DCP path we used the RODS algorithm proposed by Villà and Truhlar.[73]

Finally, for both approaches independently (MEP and DCP), this information (energies, vibrational frequencies, geometries, and gradients) was used to estimate rate constants by using variational transition state theory (VTST). We calculated thermal rates using the canonical variational theory[75,76] (CVT) approach, which locates the dividing surface between reactants and products at a point $s^{*,CVT}(T)$ along the reaction path that minimizes the generalized TST rate constants, $k^{GT}(T,s)$ for a given temperature *T*. Thermodynamically, this is equivalent to locating the transition state at the maximum $\Delta G^{GT,\circ}[T, s^{*,CVT}(T)]$ of the free energy of activation profile $\Delta G(T,s)$.[75,76] Thus, the thermal rate constant will be given by

$$K^{CVT}(T) = \sigma(k_B T/h)\, K^\circ \exp[-\Delta G(T, s^{*,CVT})/k_B T] \quad (2)$$

with k_B being Boltzmann's constant, *h* being Planck's constant, σ being the symmetry factor, and K° being the reciprocal of the standard-state concentration, taken as 1 molecule cm^{-3}.

All dynamics calculations were carried out with the general polyatomic rate constant code POLYRATE,[77] where the $^2\Pi_{1/2}$ excited state of OH in the reactant partition function (140 cm^{-1}) is correctly included. The rotational partition functions were calculated classically. The vibrations are treated as harmonic and separable, and the vibrational treatment was done using rectilinear coordinates (linear combination of Cartesian coordinates). These coordinates gave unphysical imaginary values of some lowest frequencies on the reactant and product channels, and to avoid this problem these modes were treated using the hindered-internal-rotator-approximation as implemented in POLYRATE. Moreover, for both paths (MEP and DCP) the mapped interpolation algorithm, implemented in the POLYRATE program, was used to interpolate the electronic structure information along the respective paths. Finally, the tunneling method is considered by using the centrifugal-dominant small-curvature tunneling (SCT) approach.[78]

2.2. Experimental Determination of the Rate Constant. The water soluble chemical analogue 2,3-dimethoxy-5-methyl-p-benzoquinone (coenzyme Q_0), was supplied by SIGMA Chem. Co. (Missouri). The reduced form UQ_0H_2 was prepared by chemical reduction with addition of 0.5 M $NaBH_4$ (dissolved in 0.1 M NaOH) to 20 mM coenzyme Q_0 dissolved in water (40 μL of 0.5 M $NaBH_4$ per mL of 20 mM coenzyme Q_0), and excess $NaBH_4$ was removed by treatment with HCl.[79] Reduced UQ_0H_2 solutions were purged with nitrogen for 5 min in a sealed flask and the reduction of UQ_0 was assessed from the 240−340 nm spectrum of the solution, using an extinction coefficient at 268 nm of 13.8×10^3 M^{-1} cm^{-1} for UQ_0H_2.[80] Hydroxyl radicals were generated "in situ" in the reaction mixture using the Fenton reaction, as indicated by Cohen.[81] Briefly, hydroxyl radicals were produced upon addition of hydrogen peroxide (0.2−0.5 mM) to a sodium phosphate buffered solution (pH 7.0) containing 100−150 μM diethylenetriaminepenta-acetic acid (DTPA) and 50−100 μM ferrous sulfate. In some experiments freshly prepared ascorbic acid (0.25−1 mM) was added to allow for a more sustained production of hydroxyl radicals upon ferric ions recycling to ferrous ions.[81]

The reaction of the hydroxyl radical with UQ_0H_2 was determined from the fast initial decay of the absorbance at 275 nm (once corrected for the absorbance change due to the slower oxidation of ferrous ions), which monitors the oxidation of UQ_0H_2, using an extinction coefficient of 12.25×10^3 M^{-1} s^{-1}.[82] The reaction of the hydroxyl radical with oxidized UQ_0 was determined from the kinetics of the decay of absorbance at 440 nm upon addition of ascorbic acid, slightly above the reported absorption maximum of the oxidized UQ_0 in the 400−450 nm spectral range,[83] to avoid a significant contribution of ferric salt absorption. Absorbance measurements were made with a UV−visible Shimadzu 1240 spectrophotometer, equipped with thermostated cell holders. Origin software was used to analyze the kinetic data by nonlinear least-squares fit to the first-order exponential decay equation for a first-order kinetic process:

$$A_t - A_\infty = (A_0 - A_\infty)\, e^{-k.t} \quad (3)$$

where A_0, A_t, and A_∞ are the absorbance readings at times 0, *t* and after completion of the kinetic process ($t = \infty$), and *k* is the rate constant for the first-order kinetic process.

The rate constant for the reaction of UQ_0 and UQ_0H_2 with hydroxyl radicals was determined from competition studies at 298 K using benzoate and *tert*-butanol as chemical competitors for hydroxyl radicals as indicated by Bors et al.,[84] using the following equation:

$$V_0/V = \Delta A_0/\Delta A = 1 + (k_c/k_{Q0}) \times ([C]/[\text{coenzyme } Q_0]) \quad (4)$$

where V_0 and V are the rates of the reaction in the absence and in the presence of a given concentration of the competitor, $[C]$, respectively; ΔA_0 and ΔA are the absorbance changes in the absence and in the presence of a concentration $[C]$ of the competitor; and k_c and k_{Q0} are the rate constants for the reaction of hydroxyl radicals with the competitor and the appropriate redox form of coenzyme Q_0, respectively. The values of the rate constants for the reaction between benzoate and *tert*-butanol with hydroxyl radicals at 298 K were taken as 6.0×10^9 and 0.52×10^9 M^{-1} s^{-1}, respectively.[84]

All the reagents used in this study (ascorbic acid, DTPA, ferrous sulfate, $NaBH_4$, and hydrogen peroxide) were of at least analytical grade and were supplied by either SIGMA (Missouri) or Merck (Darmstadt, Germany).

3. Results and Discussion

3.1. Experimental Rate Constants in Water Solution at pH 7. The rate constant at 298 K for the hydroxyl radical reaction with UQ_0 was determined from the dependence upon benzoate and *tert*-butanol concentrations of the kinetics of reaction after addition of hydrogen peroxide and ascorbate, monitored at 440 nm as indicated in the Methods section. It is to be noted that the absorbance at 440 nm remained constant for, at least, 5 min after the addition of ferrous sulfate and hydrogen peroxide in the absence of ascorbic acid. Thus, interference from absorbance changes due to putative ferric ion (produced during Fenton's reaction)−UQ_0 complex formation can be excluded under these experimental conditions. Benzoate and *tert*-butyl alcohol behave as competitors for the UQ_0 reaction with hydroxyl radicals, as also shown by the results in Figure 1A. The analysis of the decay of the absorbance at 440 nm indicated that this is a first-order exponential decay, and from the fit of these traces by nonlinear regression we have obtained the apparent rate constant of UQ_0 disappearance as a function of benzoate and *tert*-butanol concentrations (Figures 1B and 1C). Using the equation for competitive chemical reactions given in Bors et al.,[84] the results yielded rate constants of $(6-7) \times 10^{10}$ and $(5-7) \times 10^{10}$ M^{-1} s^{-1} for the reaction between hydroxyl radicals and UQ_0 when the chemical competitor is benzoate and *tert*-butanol, respectively. The best nonlinear fit of the data of Figures 1B and 1C gave values of the rate constant of $(6.5 \pm 0.2) \times 10^{10}$ and $(6.05 \pm 0.25) \times 10^{10}$ M^{-1} s^{-1} with benzoate and *tert*-butanol, respectively.

The rate constant for the hydroxyl radical reaction with UQ_0H_2 was determined from the dependence upon benzoate and *tert*-butanol concentrations of the extent of ubiquinol oxidation after hydroxyl radical production, measured from the fast initial decay of absorbance at 275 nm as indicated in the Methods section (which, in the absence of a competitive hydroxyl radical scavenger, amounted to 15−20% of the absorbance at 275 nm). Because the production of ferric ions through the Fenton's reaction resulted in an increase of the absorbance at 275 nm (following a slower kinetics, in the min time scale), the reaction was started by addition of hydrogen peroxide only few seconds after the addition of ferrous sulfate to minimize the interference between the two kinetic processes. The change of absorbance at 275 nm due to the slower kinetics of ferric ion formation at the time of reading the initial fast decay after addition of hydrogen peroxide (usually 15−20 s) was obtained from nonlinear regression fit of control kinetics carried out in the absence of UQ_0H_2 (results not shown), and was found to account for 5−10% of the fast initial decay measured in the absence of the competitive hydroxyl radical scavengers benzoate and *tert*-butanol. The results are shown in Figure 2, from which we

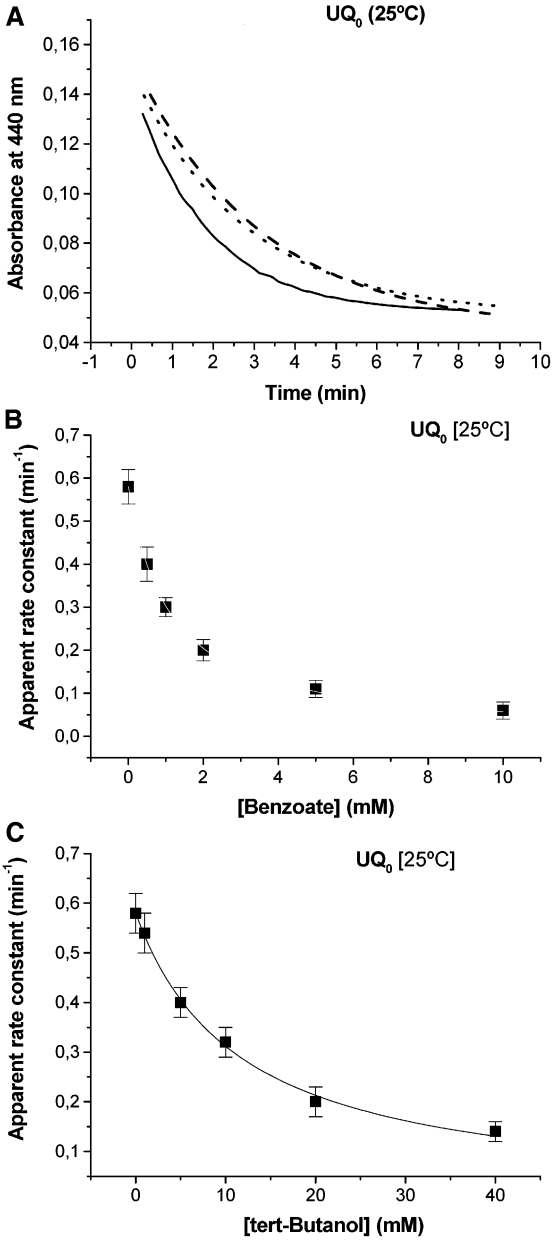

Figure 1. Experimental measurements of the reaction between hydroxyl radicals and the oxidized form of coenzyme Q_0 (UQ_0) from measurements of the kinetics of absorbance decay at 440 nm. (Panel A) Selected traces of the time course of the decay of absorbance at 440 nm at 25 °C after addition at time zero of 0.5 mM ascorbic acid to a quartz cuvette containing 100 μM UQ_0 in 50 mM sodium phosphate, 150 μM DTPA, and the concentrations of sodium benzoate or *tert*-butanol indicated below (pH 7), plus 50 μM $FeSO_4$ and 0.2 mM H_2O_2 added 1−2 min before the addition of ascorbic acid. Solid line: in the absence of chemical competitor; dotted line: in the presence of 1 mM sodium benzoate; dashed line: in the presence of 10 mM *tert*-butanol. (Panels B and C) Plot of the apparent rate constant obtained from the nonlinear least-squares fit of absorbance decay traces to the equation of a first-order kinetic process, eq 3, versus the concentration of benzoate (Panel B) and *tert*-butanol (Panel C). Each data point is the average of $n \geq 3$ independent measurements, and the error bars indicate the range of variation obtained for each experimental condition. The lines in Panels B and C are the best nonlinear least-squares fit of the experimental data to eq 4, which yielded the following values for the rate constant between hydroxyl radicals and UQ_0: $(6.5 \pm 0.2) \times 10^{10}$ M^{-1} s^{-1} ($\chi^2 = 0.00002$) (Panel B) and $(6.05 \pm 0.25) \times 10^{10}$ M^{-1} s^{-1} ($\chi^2 = 0.00008$) (Panel C).

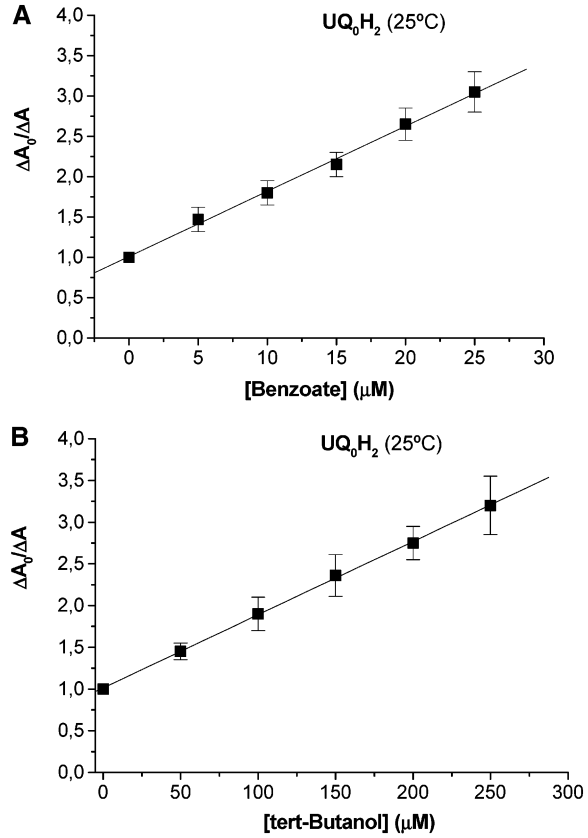

Figure 2. Experimental measurements of the reaction between hydroxyl radicals and the reduced form of coenzyme Q_0 (UQ_0H_2) from measurements of the absorbance change at 275 nm (ΔA). The absorbance change was measured at 275 nm at 25 °C after addition of 50 μM $FeSO_4$ and 0.2 mM H_2O_2 to a quartz cuvette containing 50 μM UQ_0H_2 in 50 mM sodium phosphate, 150 μM DTPA, and the concentrations of sodium benzoate or *tert*-butyl alcohol indicated below (pH 7). Panels A and B. Plot of the ratio of absorbance change ($\Delta A_0/\Delta A$) versus the concentration of benzoate (Panel A) and *tert*-butyl alcohol (Panel B). ΔA_0 ranged from 0.07 to 0.1, indicating that 10−15% of UQ_0H_2 was oxidized by hydroxyl radicals. Each data point is the average of $n \geq 3$ independent measurements, and the error bars indicate the range of variation obtained for each experimental condition. The lines in Panels A and B are the best linear least-squares fit of the experimental data to eq 4, which yielded the following values for the rate constant between hydroxyl radicals and UQ_0H_2: $(1.48 \pm 0.04) \times 10^9$ M^{-1} s^{-1} ($R = 0.9983$) (Panel A) and $(1.18 \pm 0.03) \times 10^9$ M^{-1} s^{-1} ($R = 0.9998$) (Panel B).

calculated a rate constant for the hydroxyl radical reaction with UQ_0H_2 of $(1-2) \times 10^9$ and $(0.7-1.6) \times 10^9$ M^{-1} s^{-1} with benzoate and *tert*-butanol as chemical competitors, respectively. Similar results were obtained from the fit of the kinetics when hydroxyl radicals were generated by addition of ascorbic acid as indicated in the Methods section (results not shown), except that in this case the efficiency of the UQ_0H_2 oxidation was highly improved. The best least squares linear fit of the data of Figure 2 (Panels A and B) give values of the rate constant of $(1.48 \pm 0.04) \times 10^9$ and $(1.18 \pm 0.03) \times 10^9$ M^{-1} s^{-1} with benzoate and *tert*-butanol, respectively, i.e., 1 order of magnitude lower than with the oxidized form.

3.2. Possible Pathways of Attack. In the biological membrane, both forms of coenzyme Q (ubiquinol, UQH_2, and ubiquinone, UQ) are present. When the hydroxyl radical attacks coenzyme Q, several pathways are possible, and to make the discussion clearer, we will distinguish between the two forms.

(i) In the first case, the hydroxyl radical attacking ubiquinol, UQH_2, two general pathways are possible (Scheme 3): the abstraction of the hydrogen atom from the phenolic O−H to form a "phenoxyl type" radical and water

$$UQH_2 + OH^{\bullet} \rightarrow UQH^{\bullet} + H_2O \qquad (5)$$

and the addition of the OH radical to the aromatic ring to form an adduct, in a manner similar to the reaction between atmospheric aromatic compounds and OH,[85]

$$UQH_2 + OH^{\bullet} \rightarrow UQH_2(OH)^{\bullet} \qquad (6)$$

TABLE 1: Relative Reaction Energies (ΔV_R, kcal mol^{-1}) for the CoQ + OH Reaction at the BHandHLYP/6-31G Level

approach	ΔV_R
Ubiquinol Form	
HAT	−24.3
PCET	−
ipso	+2.6
ortho-1	+3.5
ortho-2	+6.4
Ubiquinone Form	
ipso	−10.9
ortho-1	−23.6
ortho-2	−12.5

In the addition pathway, when the OH attacks ubiquinol, three approaches are possible: ipso, ortho on $-OCH_3$ (ortho-1) and ortho on $-CH_3$ (ortho-2). The relative energies with respect to the reactants (level zero) are listed in Table 1 at the BHandHLYP/6-31G level. All addition reactions are endothermic, with the more favorable approach in the order: ipso > ortho-1 > ortho-2. This endothermic behavior can be explained by the loss of bencenic ring's aromaticity with the addition.

In the hydrogen abstraction pathway, two possibilities are available, corresponding to the two orbital approaches of the OH radical to the ubiquinol molecule (Scheme 3). The first corresponds to the doubly occupied σ lone pair of the O (hydroxyl) pointing directly toward the hydrogen atom of the phenolic OH in ubiquinol. This mechanism is termed PCET (proton-coupled electron transfer)[86] in which the proton and electron are transferred between different sets of orbitals. In this reaction, the proton transfers between oxygen σ lone pairs and the electron transfers in the same direction from the doubly occupied 2p-π AO on oxygen in ubiquinol to the singly occupied 2p-π AO on the oxygen of the OH radical. Mayer et al.[86b] noted that a necessary (but not sufficient) condition for this PCET mechanism is the existence of a hydrogen bond complex prior to the transition state. We performed an exhaustive investigation of this complex over wide zones of the potential energy surface. We found a very stable hydrogen bond complex, 9.9 kcal mol^{-1} with respect to the reactants, (Scheme 4), but the orientation does not lie on the pathway to products, i.e., it is a nonproductive encounter. This complex can be explained using Mulliken population analysis (Scheme 4). Clearly, the O(ubiquinol)/H(hydroxyl) electrostatic interaction is stronger than the opposite possibility. All attempts to obtain a hydrogen bond complex for the PCET mechanism were unsuccessful at this theoretical level, and we ruled out this mechanism for the studied reaction.

The second orbital approach of the OH radical to ubiquinol corresponds to the singly occupied 2p-π AO on the oxygen in OH pointing toward the H atom of the phenolic OH in ubiquinol, following the familiar hydrogen atom transfer (HAT) mechanism of organic free radical chemistry. This pathway is strongly exothermic, −24.34 kcal mol^{-1} (Table 1) and it is the more favorable mechanism for the reduced ubiquinol form.

SCHEME 3: Schematic Representation of the Possible Pathways for the Attack of the OH Radical on Ubiquinol[a]

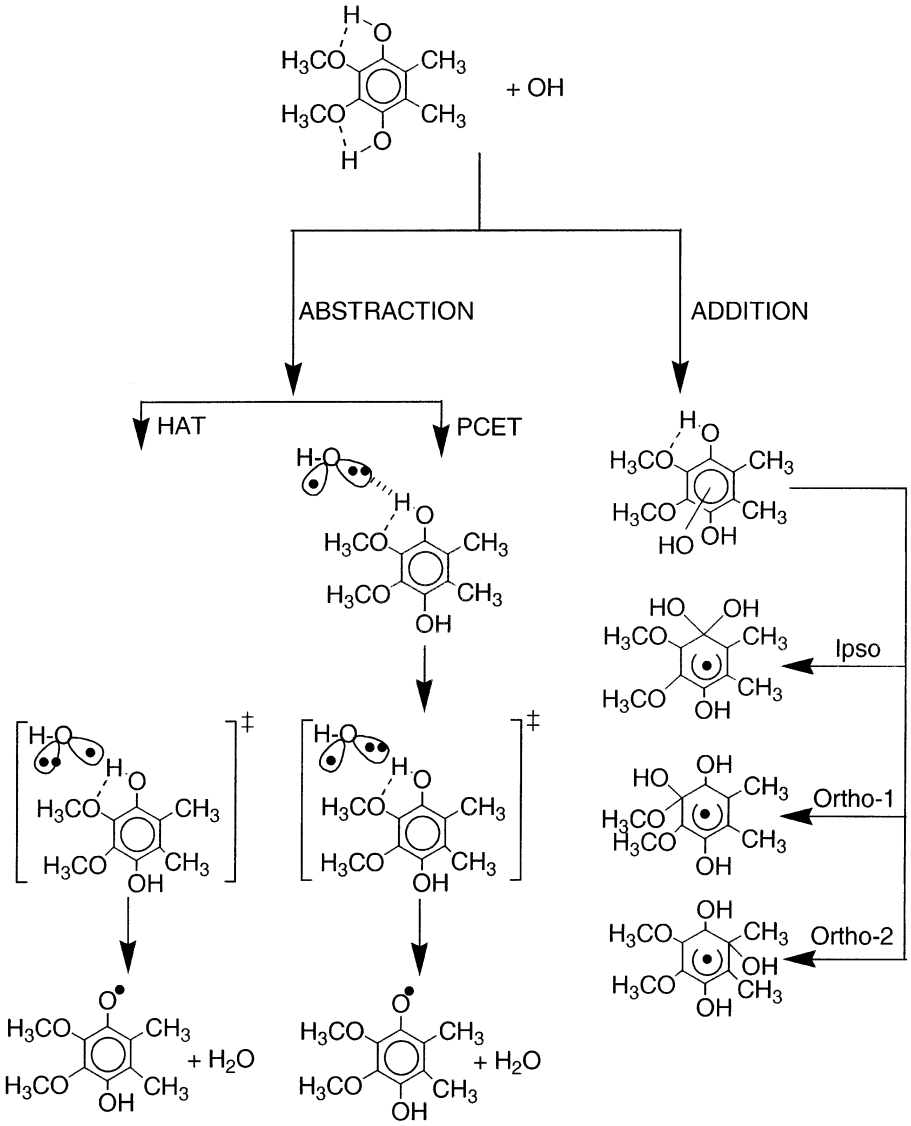

[a] HAT: hydrogen abstraction transfer; PCET: proton-coupled electron transfer; ADDITION: addition reaction on the aromatic ring

SCHEME 4: Geometry Optimized and Mulliken Population Analysis for Ubiquinol, Hydroxyl Radical, and Hydrogen Bonded Complex at the BHandHLYP/6-31G Level

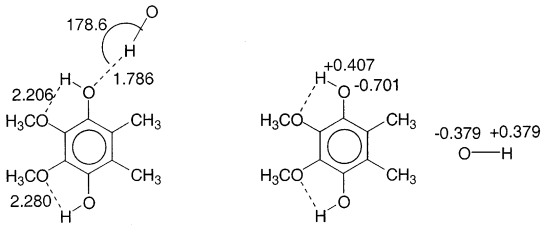

(ii) In the second case, the hydroxyl radical attacks ubiquinone, UQ, by an addition mechanism (Scheme 5). In this addition pathway, three approaches are possible: ipso, ortho on $-OCH_3$ (ortho-1) and ortho on $-CH_3$ (ortho-2). The relative energies with respect to the reactants (level zero) are also listed in Table 1 at the BHandHLYP/6-31G level. All addition reactions are exothermic, with the more favorable approach in the order: ortho-1 > ortho-2 > Ipso

At this point, we must remember that one of the major aims of this paper is to propose a mechanism to account for the attack of the OH on CoQ, i.e., hydrogen abstraction or electrophilic addition. Therefore, due to the big size of the molecular system and the great number of calculations along the respective reaction paths, in the rest of the paper we shall focus on the two most favorable pathways: the hydrogen abstraction reaction for the first case, i.e, the reaction of OH with the reduced form, ubiquinol; and the addition reaction in ortho-1 position in the second case, i.e., the reaction of OH with the oxidized form, ubiquinone. Doubtless, in view of the exothermicity of the other addition reactions on the oxidized form, these also will contribute to the final rate constant, and the ratio of the relative reaction energies (Table 1) could permit us, a priori, to establish the branching ratios.

3.3. Hydrogen Abstraction Reaction on the Reduced Form. The optimized geometries of reactant (UQH_2), product (UQH_1), and saddle point (Scheme 3), using the hybrid DFT BHandHLYP/6-31G level are shown in Figure 3. There are several geometrical features which will be analyzed following the reaction coordinate, i.e., from reactants to products. First, at the three stationary points, all six atoms directly joined to the benzene ring (i.e., two carbons and four oxygens) are in the plane of the ring, favoring electron delocalization. Second, the

SCHEME 5: Schematic Representation of the Orientations (ipso, ortho-1 and ortho-2) for the OH Addition to Ubiquinone

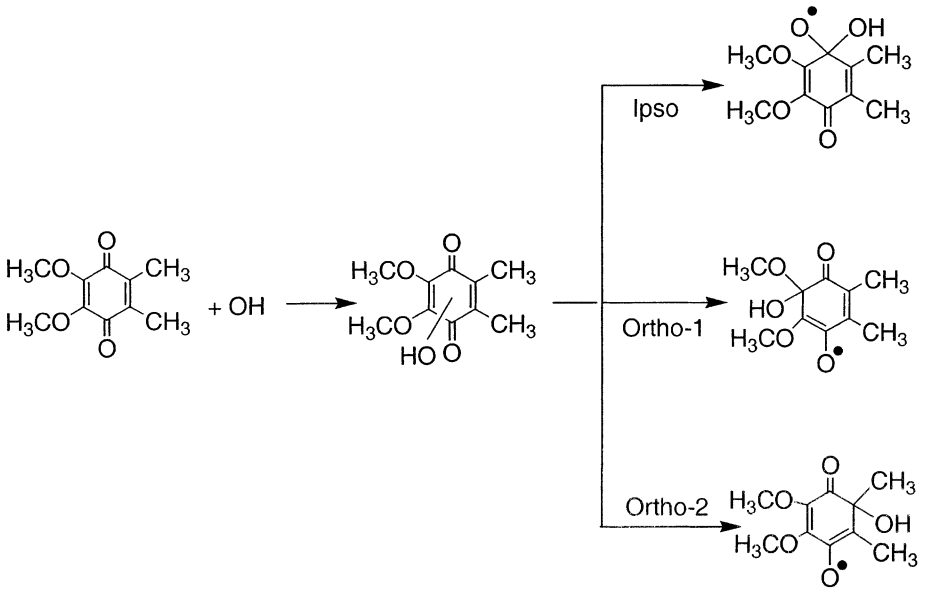

phenolic hydrogens are hydrogen bonded to the respective oxygens of the neighboring methoxy groups. Third, the two methyl substituents of the methoxy groups (ortho- and meta-) are out of the benzene plane in reactant, one above and the other below. Fourth, another interesting feature is the variation of the C−O distances, because they are related to electron delocalization along the reaction path (Figure 3). Here, for comparison purposes, we take as reference the C−O distances in methanol (single bond character: 1.435 Å) and acetone (double bond character: 1.229 Å) calculated at this same level. The C−O bonds in the ortho-methoxy groups change from 1.391 to 1.371 Å when the reaction evolves from reactants to products. These values are closer to a single bond, although some double bond character is present, i.e., they also participate in the electron delocalization. The C−O bond in the phenolic group in position "para" also presents small changes along the reaction path, from 1.379 to 1.359 Å and shows a more important double bond character. The largest changes are for the C−O bond in the phenolic group directly involved in the hydrogen abstraction, which changes from 1.379 Å in the reactant to 1.296 Å in the ubiquinoxyl radical, showing considerable double bond character. This last behavior agrees with the tendency found for the C−O bond in phenol and phenoxyl radical from experiment[87,88] or theoretical calculations,[89−93] and with the theoretical results for ubiquinol-0,[41] where the C−O bond in position para is 1.367 Å and the C−O bond directly involved in the reaction is 1.258 Å, at the B3LYP/6-31G(d,p) level.

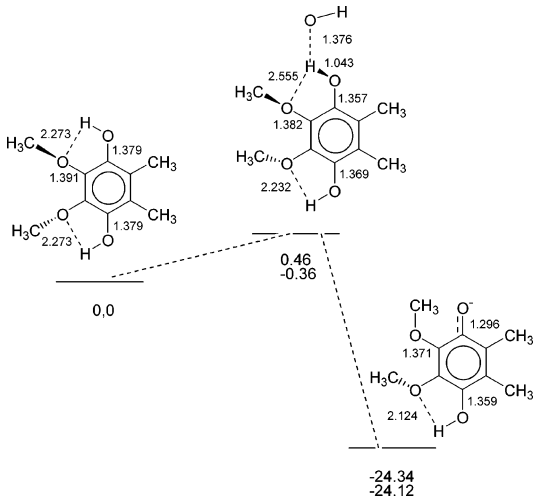

Figure 3. Reaction and barrier height energy and enthalpy at 0 K (second entry) (kcal mol^{-1}) and geometric (bond lengths in angstroms) reaction profile of the OH + ubiquinol hydrogen abstraction reaction computed at the BHandHLYP/6-31G level of theory.

At the saddle point, the most sensitive parameters are related to the breaking−forming bonds, O(phenolic)-H′ and H′-O(hydroxyl). The length of the bond that is broken increases by only 8%, while the length of the bond that is formed increases by 43%, with respect to the reactant (UQH_2) and product (H_2O) molecules, respectively. Therefore, the reaction of UQH_2 with the hydroxyl radical proceeds via an "early" transition state. This is the expected behavior that would follow from Hammond's postulate,[94] since the reaction is very exothermic (see Table 1). This saddle point was identified with one negative eigenvalue of the Hessian matrix and, therefore, one imaginary frequency (1924 i cm^{-1}).

Some authors[95−99] have postulated the existence of a complex reaction mechanism in which the oxygen-centered free radical forms a hydrogen bond complex with the HO-containing substrate. In our case, the possible complexes are HO···HOUQ, on the reactant channel, and HOH···OUQ, on the product channel. For this reaction, several hydrogen bonded complexes were searched, in both reactant and product valleys in two independent ways. On one hand, we followed the conventional method of approaching the two subsystems from infinity, and, on the other hand, we followed the IRC starting from the saddle point and going downhill to both reactant and product channels. All attempts to locate these complexes were unsuccessful at this theoretical level. We found only a hydrogen bond complex where the hydrogen of the attacking hydroxyl radical is hydrogen bonded to the phenolic oxygen, i.e., OH···OHUQ, (Scheme 4). Clearly, this orientation will give a nonproductive encounter because it is not on the reaction path to the products.

Finally, the energy and enthalpy (0 K) changes (reaction and activation) are also plotted in Figure 3. Note that the enthalpic nomenclature, $\Delta H_o°$, is equivalent to that used in eq 1, ΔV_a^G. Unfortunately, comparison with experimental or theoretical work is not possible, because the enthalpy of reaction has been directly

measured neither experimentally nor theoretically. However, an estimate of this value is possible by considering that the enthalpy of reaction, $\Delta H_o°$, is the difference between the bond dissociation energies [BDE(O−H)] of the bonds broken and formed:

$$\Delta H_o° = \mathrm{BDE}(\mathrm{UQH_2}) - \mathrm{BDE}(\mathrm{H_2O}) \qquad (7)$$

Taking the BDE(H_2O) = 117.90 kcal mol^{-1} and BDE(UQH_2) = 78.5 ± 1.5 kcal mol^{-1} from literature,[41,100] a value of $\Delta H_o°$ = −38.00 kcal mol^{-1} is proposed for the studied reaction (Figure 3). Thus, our results qualitatively describe the exothermic character of this reaction. It is well-known that a major source of errors of standard theoretical calculations of molecular energies arises from the truncation of the one electron basis set. Thus, to estimate the limitations, we performed calculations of the reaction energy and barrier height using larger basis sets, namely, 6-31G(d,p) and 6-311+G(d,p). For the enthalpy of reaction (0 K) we obtained values of −28.32 and −30.00 kcal mol^{-1}, respectively. Clearly, larger the basis is, the better the agreement with experiment. Note, however, that even with a basis set large enough for this molecular system, the difference is of 8 kcal mol^{-1}. With respect to the barrier height, the values are 1.86 and 3.17 kcal mol^{-1}, respectively (1.04 and 2.35 kcal mol^{-1} for the enthalpy (0K) change), i.e., higher than those obtained with the 6-31G basis set. On the other hand, to estimate the influence of the functional used, we also performed also energetic calculations (reaction and activation) using a different functional: B3LYP/6-31G. We obtained an enthalpy of reaction (0 K) of −32.00 kcal mol^{-1}, in better agreement with experiment. However, all attemps to locate the saddle point at this level were unsuccessful, and therefore, we discarded this level in our study.

In summary, a better agreement with experiment could only be possible when more complete correlation energy methods and larger basis sets were used, which is beyond of the scope of this work given the large size of the molecular system.

3.4. Addition to Ubiquinone. The optimized geometries of all stationary points (reactants and adducts) and the energy and enthalpy (0 K) changes at the BHandHLYP/6-31G level are shown in Figure 4. Several geometrical features need emphasizing. First, while in ubiquinone all six atoms directly joined to the benzene ring (i.e., two carbons and four oxygens) are in the plane of the ring, the addition of the OH free radical to form the adducts (ipso, ortho-1, and ortho-2) breaks this planarity on the reactive center. Second, when the OH attacks ubiquinone, the spin density is located in different oxygen atoms, changing their C−O distances. Thus, for the ipso approach, the spin density is located on the oxygen in ipso, which changes its C−O distance from 1.244 Å in ubiquinone to 1.452 Å in the adduct, i.e., practically a single bond. For the ortho-1 and ortho-2 approaches, the spin density is located on the oxygen in position "para", which changes the C−O distance only slightly, retaining the double bond character. Third, another interesting feature is the value of the new C−O bond formed with the OH attack. While in the ipso approach it is practically a single bond, in the ortho-1 and ortho-2 approaches it is weaker than a single bond.

For the most favorable approach, OH on the ortho-1 position, the new C−O bond formed with the OH attack is chosen as a distinguished coordinate to define the DCP path. The C−O distance ranges from 3.0 to 1.5 Å. This reaction proceeds directly from reactants to the adduct, without an intermediate saddle point. This behavior is typical of radical addition reactions, which are very fast, practically barrierless, and present inverse temperature dependence of the rate constants, i.e., negative

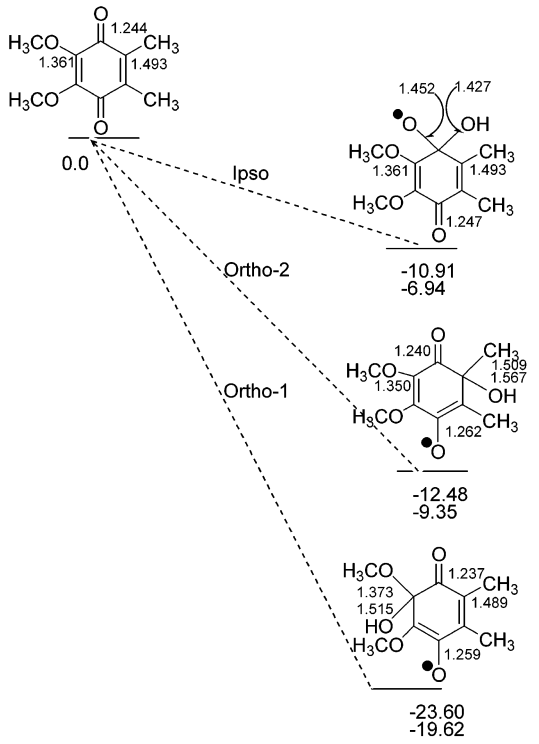

Figure 4. Reaction energy and enthalpy at 0 K (second entry) (kcal mol^{-1}) and geometric (bond lengths in angstroms) reaction profiles of the three orientations (ipso, ortho-1, and ortho-2) for the OH + ubiquinone addition reaction computed at the BHandHLYP/6-31G level of theory.

activation energy. The other two approaches (ortho-2 and ipso) would be expected to evolve in a similar way, although they were not calculated in this work.

3.5. Theoretical Rate Constant Calculations. As indicated in the Methods section, the reaction path and reaction valley information was obtained in different ways for the different approaches. Thus, for the hydrogen abstraction reaction on ubiquinol, the MEP was constructed starting from the saddle point; while for the addition reaction in ortho-1 position on ubiquinone, the DCP was constructed choosing the new C−O bond formed as distinguished coordinate. Since in our model reaction the isoprenoid "tail" was replaced by a methyl group, the two phenolic abstractable hydrogens in ubiquinol and the two carbons in ortho-1 positions in ubiquinone are respectively equivalent, and the respective total rate constants were calculated by considering the rate constant for one abstraction reaction and one addition reaction, respectively, and multiplying by 2.

As we noted above, the reaction of CoQ with the hydroxyl radical can proceed via two pathways: hydrogen abstraction on ubiquinol and addition reaction on ubiquinone. They are therefore two competitive reactions. Therefore, the total rate constant will be

$$k(T) = k^{\mathrm{abs}}(T) + k^{\mathrm{add}}(T) \qquad (8)$$

For the hydrogen abstraction reaction on ubiquinol, Table 2 lists the canonical variational rate constants (CVT) for the temperature range 200−500 K, together the experimental values at 298 K for comparison. (Note that this range is very wide for a biological system, but it permits us a clearer interpretation of the temperature dependence of the rate constants). The bottleneck properties of the reaction, based on the CVT approach, show that the location of the generalized transition state (GTS) is always at the saddle point over all temperature range. Thus,

TABLE 2: Theoretical and Experimental Rate Constants (k, M^{-1} s^{-1}) as a Function of Temperature

	theoretical[a]		experimental	
T (K)	abstraction	addition	UQ_0H_2	UQ_0
200	3.71(8)[b]	6.62(11)		
250	3.06(8)	8.07(10)		
298	2.84(8)	2.14(10)	$1.3 \pm 0.2(9)$	$6.25 \pm 0.25(10)$
300	2.83(8)	2.04(10)		
350	2.80(8)	8.01(9)		
400	2.86(8)	4.06(9)		
450	3.00(8)	2.47(9)		
500	3.18(8)	1.70(9)		

[a] Canonical variational CVT rate constants at the BHandHLYP/6-31G level. [b] 3.71(8) stands for $3.71 \times 10^{+8}$, in M^{-1} s^{-1}.

the variational effects on the thermal rate constants are negligible, i.e., the free energy maximum occurs at the saddle point, indicating that the classical potential energy contribution predominates over the entropy contribution. Note that the variational effect is defined as the ratio between the variational CVT and conventional TST rate constants. For the tunneling contribution, as information is only available on the reaction path, the centrifugal-dominant small-curvature (SCT)[78] method was used. As the adiabatic barrier for this hydrogen abstraction reaction presents a negative value (see Figure 3), the tunneling correction has a value unity at all temperatures. At 298 K, the theoretical rate constant is slightly lower than the experimental values (also determined in this work).

For the addition reaction in the ortho-1 position on ubiquinone, the CVT rate constants are also listed in Table 2. As noted previously, calculations using the optimized geometries from the DCP approach provide a reaction path as a function of the new C−O bond formed, which presents neither a classical nor an adiabatic potential energy barrier. At 298 K the theoretical rate constant is of the same order of magnitude as the experimental values.

The agreement between theory and experiment for the two pathways, abstraction and addition, lends confidence to the theoretical level and model used. Moreover, as theoretically as experimentally, the OH addition to ubiquinone is 10−100 times faster than the hydrogen abstraction reaction on ubiquinol, and therefore the addition mechanism seems the most favorable mechanism in a molecule-per-molecule ratio.

The total rate constants can be obtained by taking into account both mechanisms (abstraction and addition, eq 8), but due to the differences between the two values (about 2 orders of magnitude) the total rate constants practically coincide with the addition mechanism values. The differences with the experimental data can be explained by the limitations of this study model: the other addition approaches (ipso and ortho-2) on ubiquinone should also be taken into account, the gas-phase environment used, the modeling of the real system, etc.

The calculated rate constants show a negative temperature dependence and, consequently, a negative activation energy, which is the expected behavior for a free radical addition reaction. Activation energies can be obtained from rate constants through the usual definition

$$E_a = -R\frac{d(\ln k)}{d(1/T)} \tag{9}$$

which is equivalent to determining the slope of the plot of ln k versus $1/T$. At 298 K, a value of -4.0 kcal mol^{-1} is found.

The experimental rate constant of the reaction between hydroxyl radicals and UQ_0 was measured at pH 7 at 25 and 55 °C from the kinetics of decay of the absorbance at 440 nm as indicated in the Methods section and in the legend to Figure 1A. The experimental values obtained for the apparent rate constant of UQ_0 oxidation at 25 and 55 °C were found to be 0.58 ± 0.06 and 0.19 ± 0.02 min^{-1}, respectively, which leads to an experimental value for the activation energy of -7.4 ± 1.3 kcal/mol, in good agreement with the theoretical prediction of a negative activation energy for this reaction. These theoretical and experimental results seem also to point toward the addition mechanism proposed in this work.

To understand the behavior of this negative activation energy, we analyzed the Gibbs free energy variation with T, which can be decomposed into enthalpy and entropy contributions:

$$\Delta G^{GT,0} = \Delta H^{GT,0} - T\Delta S^{GT,0} \tag{10}$$

where

$$\Delta H^{GT,0} = RT^2\frac{d \ln k^{CVT}}{dT} - 2RT \tag{11}$$

and

$$-T\Delta S^{GT,0} = \Delta G^{GT,0} - \Delta H^{GT,0} \tag{12}$$

These equations are equivalent to those employed previously,[101] and the standard state for all equations is the ideal gas state at 1 atm. In practice, the derivatives in eq 11 were calculated by a two-point central difference algorithm. Thus, at 298 K, $\Delta H^{GT,0}$ is -5.2 kcal mol^{-1}, while $-T\Delta S^{GT,0}$ is $+37.3$ kcal mol^{-1}.

At this point it is useful to consider the following relationship between the activation energy and the enthalpy change corresponding to the variational transition state:

$$E_a = \Delta H^{GT,0} + 2RT \tag{13}$$

which holds for bimolecular chemical reactions in the gas phase (provided that no tunneling effect exists) and is also derived by using the van't Hoff equation.[101,102] At a given temperature, the value of E_a depends on the balance between the term $\Delta H^{GT,0}(T)$ and $2RT$ according to eq 13. The value obtained at 298 K, $\Delta H^{GT,0}(298\ K) = -5.2$ kcal mol^{-1}, becomes large enough in absolute value to overcome the positive 2RT term (1.2 kcal mol^{-1}), producing a negative activation energy. Therefore, with this explanation of the activation energy we ruled out the need for a pre-reactive complex in the entry channel to explain the negative tendency of this magnitude.

3.6. Comparison with Analogous Systems. Interestingly, this addition mechanism is supported by the experimental evidence in analogous reactions. First, this reaction shows the behavior of general unsaturated compounds with the OH radical. It is well known that at low temperatures ($T < 500$ K) these reactions are dominated by the electrophilic addition of OH to the unsaturated compound to form an adduct, while at higher temperatures ($T > 750$ K) the abstraction of a hydrogen atom becomes the preferred mechanism.[2] Unfortunately, the experimental information including both mechanisms for the same unsaturated compound is very scarce. Some values in the gas-phase are listed in Table 3, together with our theoretical calculations for the CoQ + OH reaction. Note that the addition/abstraction ratio of several unsaturated compounds with OH (including the title reaction) show a range of 10^1-10^3. In general, it is admitted that at room temperature the H atom abstraction represents <10% of the overall OH radical reaction[104] and that the addition reaction is very fast, with most

TABLE 3: Addition/Abstraction Rate Constants for Several Unsaturated Compounds with OH in the Gas Phase, at 298 K, in M^1 s^{-1}

	rate constant		
unsaturated compound[a]	addition	abstraction[b]	ratio[c]
C_2H_4	5.4(9)	9.0(5)	10^3
C_3H_6	1.8(10)	1.5(8)	10^2
C_6H_6	7.2(8)	4.5(7)	10^1
$C_6H_5-CH_3$	1.3(9)	1.1(6)	10^3
$p-C_6H_4(CH_3)_2$	8.4(9)	3.1(8)	10^1
CoQ	2.1(10)	2.8(8)	10^2

[a] Reference 103. [b] Extrapolated values from higher temperature range. [c] Order of magnitude of the addition/abstraction ratio.

TABLE 4: Mechanism and Rate Constants for Several Biological Compounds with OH, at 298 K, in M^1 s^{-1}

compound	mechanism	rate constant	ref
thymine	addition	1.7(9)	105, 106
uracil	addition	2.6(9)	105
guanine	addition		106
NADH[a]	addition	2.0(10)	107
melatonin	addition	2.7(10)	108, 109
CoQ	addition	6.25(10)	this work
IPA[b]	?	7.8(10)	110

[a] Nicotinamide adenine dinucleotide. [b] Imidole-3-propionate.

rate constants within 1 order of magnitude of the diffusion-controlled limit.[2]

Second, the addition mechanism is a common pathway for other biological systems. Table 4 lists some systems together with the title reaction at room temperature. All systems present a strong scavenging activity with respect to the OH radical, with very high rate constants, that are practically diffusion-controlled.

4. Concluding Remarks

The results obtained in this study allow us to conclude that coenzyme Q is one of the most reactive molecules against hydroxyl radicals present in mammalian cells, because to the best of our knowledge the experimental bimolecular reaction constant at 298 K in aqueous solution at pH 7.0 between oxidized UQ_0 and hydroxyl radicals, 6.25×10^{10} M^{-1} s^{-1} [acceptable experimental interval $(4-7) \times 10^{10}$ M^{-1} s^{-1}] is one of the highest reported so far for the reaction between hydroxyl radicals and relevant biochemical molecules in mammalian cells (see Table 4). Moreover, assuming a value for the diffusion coefficient of hydroxyl radicals in water close to twice that of oxygen, considering the molecular shape and size of the oxidized form of coenzyme Q_0 the value we obtained experimentally for the rate constant of the reaction between hydroxyl radicals and UQ_0 is close to the collisional diffusion rate constant that can be calculated for this reaction using the Smoluchowski equation. In addition, it is also remarkable that the relative chemical reactivity of UQ_0 and UQ_0H_2 against hydroxyl radicals measured experimentally and predicted on theoretical grounds is within the acceptable experimental range, as shown by the ratio between the rate constants for the reaction of hydroxyl radicals with UQ_0 and UQ_0H_2 (R) obtained from experimental data ($R_{exp} = 25-100$) and that from theoretical calculations ($R_{theo} = 72$). Whether this conclusion may apply to other reactions of hydroxyl radicals (or other highly reactive radicals) with rate constants close to the collisional diffusion rate deserves to be established. Regarding coenzyme Q, considering the very different chemical environments to obtain both sets of data (diluted gas phase for theoretical calculations and liquid water phase for experimental measurements), this result suggests that the reactivity of coenzyme Q with hydroxyl radicals should not be highly dependent on the partition of coenzyme Q into the lipid phase within the cells.

There has been considerable experimental effort directed at understanding the role of antioxidants in biological processes and cell survival, which contrasts with the paucity of theoretical studies. In the present paper, by employing a direct dynamics method, we were able, for the first time, to study the kinetics and dynamics of this antioxidant process using a prototype of coenzyme Q with the hydroxyl radical in the gas-phase.

The OH radical can attack coenzyme Q by different pathways, and we found that the most favorable mechanisms are the hydrogen abstraction reaction from the phenolic hydrogen on the reduced form (ubiquinol), and the electrophilic OH addition on the oxidized form (ubiquinone). Both mechanisms are strongly exothermic ($\approx$20 kcal mol^{-1}), the first with a low barrier height ($\approx$0.5 kcal mol^{-1}), while the second is a barrierless reaction. The equilibrium structures of all stationary points and the reaction valleys for both mechanisms were analyzed using hybrid density functional theory at the BHandHLYP/6-31G level.

The rate constants for each mechanism were independently calculated by using the variational transition-state theory with multidimensional tunneling. We found that the $^{\bullet}$OH addition mechanism on ubiquinone is responsible for the overall rate constant and the value agrees with the experimental data, also obtained in this work. These final rate constants present a negative temperature dependence, leading to a negative activation energy. This negative value for this barrierless reaction is due to the negative value of the enthalpy associated with the generalized transition state, where the tunneling effect is negligible.

Theoretical calculations indicate that the reaction of ubiquinol and ubiquinone with hydroxyl radicals leads to intermediate states of coenzyme Q that should have different reduction potentials. Because in living cells coenzyme Q functions as an obligatory intermediate electron carrier in mitochondria[24] or plasma membrane[26] redox chains, impairment of its recycling to the reduced state will result in at least partial loss of its biological activity. In this regard, it is to be noted that the intermediate state of coenzyme Q attained after the reaction of ubiquinone with hydroxyl radicals would not be expected to be reduced by ascorbic acid, which is one of the major electron donors for "in vivo" reduction of the oxidized form of coenzyme Q.[26,29] Thus, hydroxyl radicals are expected to be more damaging to biological functions performed by coenzyme Q when these radicals are produced in cells where the equilibrium between reduced and oxidized coenzyme Q is significantly displaced toward the oxidized form. A shift of the equilibrium between reduced and oxidized coenzyme Q toward the oxidized form is likely to be produced "in vivo" as a result of the large cellular oxidative stress associated to inflammation and to the ischaemia-reperfusion syndrome linked with cardiovascular dysfunction.[8,9]

Acknowledgment. We are grateful to Prof. Donald G. Truhlar for providing a copy of the POLYRATE program, to Dr. José C. Corchado for computational support, and to the Consejeria de Educación, Ciencia y Tecnología, Junta de Extremadura (Spain) (Projects No. 2PR01A002 and IPR00A091) for partial financial support of this work.

References and Notes

(1) Perry, R. A.; Atkinson, R.; Pitts, J. N. *J. Chem. Phys.* **1976**, *64*, 3237 and references therein.

(2) Atkinson, R. *Chem. Rev.* **1986**, *86*, 69 and references therein.
(3) Meyer, L. S.; Kay, E. *Int. J. Radiat. Oncol. Biol. Phys.* **1979**, *5*, 1055.
(4) Adams, G. E. *Adv. Radiat. Chem.* **1972**, *3*, 125.
(5) Wilson, R. R. In *Oxygen free radicals and tissue damage*, CIBA Foundations Symposium 65; Excerpta Medica: Amsterdam, 1979; p 19−42.
(6) *Free Radicals in Biology*; Pryor, W. A., Series Ed.; Academic Press: beginning 1976.
(7) *CRC Handbook of Methods for Oxygen Radical Research*; Greenwald, R. A., Ed.; CRC Press Inc.: Boca Raton, Florida, 1984.
(8) Darley-Usmar, V.; Wiseman, H.; Halliwell, B. *FEBS Lett.* **1995**, *369*, 131.
(9) Halliwell, B.; Gutteridge, J. M. C. *Free Radicals in Biology and Medicine*; Clarendon Press: Oxford, U.K., 1999.
(10) Harman, D. *J. Am. Geriatr. Soc.* **1972**, *20*, 145.
(11) Salvioli, S.; Bonafé, M.; Capri, M.; Monti, D.; Franceschi, C. *FEBS Lett.* **2001**, *492*, 9.
(12) Stocker, R. *Trends Biochem. Sci.* **1999**, *24*, 219.
(13) Ernster, L.; Dallner, G. *Biochim. Biophys. Acta* **1995**, *1271*, 195.
(14) Forsmark-Andrée, P.; Dallner, G.; Ernster, L. *Free Rad. Biol. Med.* **1995**, *19*, 749.
(15) Wolf, G. *Nutr. Rev.* **1997**, *55*, 376.
(16) Tokumaru, S.; Ogino, R.; Shiromoto, A.; Iguchi, H.; Kojo, S. *Free Rad. Res.* **1997**, *26*, 169.
(17) Pryor, W. A. *Free Rad. Biol. Med.* **2000**, *28*, 141.
(18) Mellors, A.; Tappel, A. I. *J. Biol. Chem.* **1966**, *241*, 4353.
(19) Takayanagi, R.; Takashige, K.; Minakami, S. *Biochem. J.* **1980**, *192*, 853.
(20) Marubayashi, S.; Dohi, K.; Yamada, Y.; Kawasaki, T. *Biochim. Biophys. Acta* **1984**, *797*, 1.
(21) Stocker, R.; Bowry, V. W.; Frei, B. *Proc. Natl. Acad. Sci. U.S.A.* **1991**, *88*, 1646.
(22) Mohr, D.; Bowry, V. W.; Stocker, R. *Biochim. Biophys. Acta* **1992**, *1126*, 247.
(23) White, A.; Hadler, P.; Smith, E. L. *Biochemistry*; McGraw-Hill Kogakuska: Tokyo, 1968; p 323.
(24) Zubay, G. *Biochemistry*; Addison-Wesley: Reading, MA, 1983.
(25) Lenaz, G. *FEBS Lett.* **2001**, *509*, 151.
(26) May, J. M. *FASEB J.* **1999**, *13*, 995.
(27) Villalba, J. M.; Navarro, F.; Córdoba, F.; Serrano, A.; Arroyo, A.; Crane, F. L.; Navas, P. *Proc. Natl. Acad. Sci. U.S.A.* **1995**, *92*, 4887.
(28) Martín-Romero, F. J.; Gutiéreez-Martín, Y.; Henao, F.; Gutiérrez-Merino, C. *J. Neurochem.* **2002**, *82*, 604.
(29) Winkler, B. S. *Biochim. Biophys. Acta* **1992**, *1117*, 287.
(30) Schafer, F. Q.; Buettner, G. R. *Free Rad. Biol. Med.* **2001**, *30*, 1191.
(31) Chandra, J.; Samali, A.; Orrenius, S. *Free Rad. Biol. Med.* **2000**, *29*, 323.
(32) Walling, C. *Free Radicals in Solution*; Wiley: New York, 1957.
(33) Ingold, K. U. *Acc. Chem. Res.* **1969**, *2*, 1.
(34) Barclay, L. R. C.; Vinqvist, M. R.; Mukai, K.; Itoh, S.; Morimoto, H. *J. Org. Chem.* **1993**, *58*, 7416.
(35) Ingold, K. U.; Bowry, V. W.; Stocker, R.; Walling, C. *Proc. Natl. Acad. Sci. U.S.A.* **1993**, *90*, 45.
(36) Foti, M.; Ingold, K. U.; Lusztyk, J. *J. Am. Chem. Soc.* **1994**, *116*, 9440.
(37) Avila, D. V.; Ingold, K. U.; Lusztyk, J.; Green, W. H.; Procopio, D. R. *J. Am. Chem. Soc.* **1995**, *117*, 2929.
(38) Valgimigli, L.; Banks, J. T.; Ingold, K. U.; Lusztyk, J. *J. Am. Chem. Soc.* **1995**, *117*, 9966.
(39) MacFaul, P. A.; Ingold, K. U.; Lusztyk, J. *J. Org. Chem.* **1996**, *61*, 1316.
(40) Nagaoka, S.; Nishioki, Y.; Mukai, K. *Chem. Phys. Lett.* **1998**, *287*, 70.
(41) de Heer, M. I.; Korth, H.-G.; Mulder, P. *J. Org. Chem.* **1999**, *64*, 6969.
(42) Bowry, V. W.; Ingold, K. U. *Acc. Chem. Res.* **1999**, *32*, 27.
(43) de Heer, M. I.; Mulder, P.; Korth, H.-G.; Ingold, K. U.; Lusztyk, J. *J. Am. Chem. Soc.* **2000**, *122*, 2355.
(44) Naumov, V. V.; Khrapova, N. G. *Biofizika* **1983**, *28*, 730.
(45) Yamamoto, Y.; Komouro, E.; Niki, E. *J. Nutr. Sci. Vitaminol.* **1990**, *36*, 505.
(46) Kagan, V.; Serbinova, E.; Packer, L. *Biochem. Biophys. Res. Commun.* **1990**, *169*, 851.
(47) Wayner, D. D. M.; Lusztyk, E.; Ingold, K. U.; Mulder, P. *J. Org. Chem.* **1996**, *61*, 6430.
(48) Türker, L. *Models Chem.* **2000**, *137*, 701.
(49) Deward, M. J. S.; Zoebish, E. G.; Healey, E. F.; Steward, J. J. P. *J. Am. Chem. Soc.* **1985**, *107*, 3902.
(50) Aberg, F.; Appelkvist, E. L.; Dallner, G.; Ernter, L. *Arch. Biochem. Biophys.* **1992**, *295*, 230.
(51) Ross, A. B.; Bielski, B. H. J.; Buxton, G. V. *NIST Standard Reference Database 40. NDRL/NIST solution kinetic database*; NIST: Gaithersburg. MD, 1992.
(52) Frisch, M. J.; Trucks, G. W.; Schlegel, H. B.; Scuseria, E.; Robb, M. A.; Cheeseman, J. R.; Zakrzewski, V. G.; Montgomery, J. A.; Stratman, R. E.; Burant, J. C.; Dapprich, S.; Millam, J. M.; Daniels, A. D.; Kudin, K. N.; Strain, M. C.; Farkas, O.; Tomasi, J.; Barone, V.; Cossi, M.; Cammi, R.; Menucci, B.; Pomelli, C.; Adamo, C.; Clifford, S.; Ochterki, J.; Petterson, G. A.; Ayala, P. Y.; Cui, Q.; Morokuma, K.; Malik, D. K.; Rabuk, A. D.; Raghavachari, K.; Foresman, J. B.; Cioslowski, J.; Ortiz, J. V.; Stefanov, J. J.; Liu, G.; Liashenko, A.; Piskorz, P.; Komaromi, I.; Gomperts, R.; Martin, R. L.; Fox, D. J.; Keith, T.; Al-Laham, M. A.; Peng, C. Y.; Nanayakkara, A.; González, C.; Challacombe, M.; Gill, P. M. W.; Johnson, B. G.; Chen, W.; Wong, M. W.; Andres, J. L.; Head-Gordon, M.; Reploge, E. S.; Pople, J. A. *GAUSSIAN98 program*, revision A.7; Gaussian Inc.: Pittsburgh, PA, 1998.
(53) Becke, A. D. *J. Chem. Phys.* **1993**, *98*, 1372.
(54) Lee, C.; Yang, W.; Parr, R. G. *Phys. Rev. B* **1988**, *37*, 785.
(55) Truong, T. N.; Duncan, W. *J. Chem. Phys.* **1994**, *101*, 7403.
(56) Zhang, Q.; Bell, R.; Truong, T. N. *J. Phys. Chem.* **1995**, *99*, 592.
(57) Durant, J. L. *Chem. Phys. Lett.* **1996**, *256*, 595.
(58) Lynch, B. J.; Fast, P. L.; Harris, M.; Truhlar, D. G. *J. Phys. Chem. A* **2000**, *104*, 4811.
(59) Baker, J.; Scheiner, A.; Andzelm, J. *Chem. Phys. Lett.* **1993**, *216*, 380.
(60) Erikson, L. A.; Malkina, O. L.; Malkin, V. G.; Salahub, D. R. *J. Chem. Phys.* **1994**, *100*, 5066. (b) Wang, J.; Becke, A. D.; Smith, V. H. *J. Chem. Phys.* **1995**, *102*, 3477. (c) Laming, G. J.; Handy, N. C.; Amos, R. D. *Mol. Phys.* **1993**, *80*, 1121.
(61) Doubleday, C. J.; McIver, J. W.; Page, M. *J. Chem. Phys.* **1988**, *92*, 4367.
(62) Baldridge, K. M.; Gordon, M. S.; Steckler, R.; Truhlar, D. G. *J. Phys. Chem.* **1989**, *93*, 5107.
(63) Espinosa-García, J.; Corchado, J. C.; Truhlar, D. G. *J. Am. Chem. Soc.* **1997**, *119*, 9891.
(64) Corchado, J. C.; Espinosa-García, J.; Roberto-Neto, O.; Chang, Y.-Y.; Truhlar, D. G. *J. Phys. Chem.* **1998**, *102*, 4899.
(65) Espinosa-García, J.; Corchado, J. C. *J. Chem. Phys.* **2000**, *112*, 5731.
(66) Corchado, J. C.; Truhlar, D. G.; Espinosa-García, J. *J. Chem. Phys.* **2000**, *112*, 9375.
(67) González-Lafont, A., Lluch, J. M.; Espinosa-García, J. *J. Phys. Chem. A* **2001**, *105*, 10553.
(68) Espinosa-García, J. *J. Chem. Phys.* **2002**, *116*, 10664.
(69) Espinosa-García, J. *J. Chem. Phys.* **2002**, *117*, 2076.
(70) Espinosa-García, J. *J. Phys. Chem. A* **2003**, *107*, 1618.
(71) Villá, J.; González-Lafont, A.; Lluch, J. M.; Corchado, J. C.; Espinosa-García, J. *J. Chem. Phys.* **1997**, *107*, 7266.
(72) Miller, W. H.; Handy, N. C.; Adams, J. E. *J. Chem. Phys.* **1980**, *72*, 99. (b) Morokuma, K.; Kato, S. In *Potential Energy Surfaces and Dynamics Calculations*; Truhlar, D. G., Ed.; Plenum Publishing: New York, 1981; p 243. (c) Kraka, E.; Dunning, T. H. In *Advances in Molecular Electronic Structure Theory*; JAI: New York, 1990; Vol. I, p 129.
(73) Villà, J.; Truhlar, D. G. *Theor. Chim. Acta* **1997**, *97*, 317.
(74) Chen, Z. *Theor. Chim. Acta* **1989**, *75*, 481.
(75) Garrett, B. C.; Truhlar, D. G. *J. Am. Chem. Soc.* **1979**, *101*, 4354.
(76) Truhlar, D. G.; Isaacson, A. D.; Garrett, B. C. In *The Theory of Chemical Reaction*; Baer, M., Ed.; Chemical Rubber: Boca Raton, Florida,, 1985; Vol. 4.
(77) Chuang, Y. Y.; Corchado, J. C.; Fast, P. L.; Villá, J.; Coitiño, E. L.; Hu, W. P.; Liu, Y. P.; Lynch, G. C.; Nguyen, K.; Jackells, C. F.; Gu, M. Z.; Rossi, I.; Clayton, S.; Melissas, V.; Steckler, R.; Garrett, B. C.; Isaacson, A. D.; Truhlar, D. G. *POLYRATE* Version 8.4; University of Minnesota: Minneapolis, 1999.
(78) Lu, D. H.; Truong, T. N.; Melissas, V. S.; Lynch, G. C.; Liu, Y. P.; Garrett, B. C.; Steckler, R.; Isaacson, A. D.; Rai, S. N.; Hancock, G. C.; Lauderdale, G. C.; Joseph, Y.; Truhlar, D. G. *Comput.Chem. Commun.* **1992**, *71*, 235.
(79) Cadenas, E.; Boveris, A.; Ragan, C. I.; Stoppani, A. O. M. *Arch. Biochem. Biophys.* **1977**, *180*, 248.
(80) Degli Esposti, M.; Ngo, A.; McMullen, L.; Ghelli, A.; Sparla, F.; Benelli, B.; Ratta, M.; Linnane, A. *Biochem. J.* **1996**, *313*, 327.
(81) Cohen, G. In *Handbook of Methods for Oxygen Radical Research*; Greenwald, R. A., Ed.; CRC Press: Boca Raton, Florida, 1985; p 55−64.
(82) Redfearn, E. R. *Methods Enzymol.* **1967**, *10*, 381.
(83) Schöpfer, F.; Riobó, N.; Carreras, M. C.; Alvarez, B.; Radi, R.; Boveris, A.; Cadenas, E.; Poderoso, J. J. *Biochem. J.* **2000**, *349*, 35.
(84) Bors, W.; Michel, C.; Saran, M. In *Handbook of Methods for Oxygen Radical Research*; Greenwald, R. A., Ed.; CRC Press: Boca Raton, Florida, 1985; p 181−188.
(85) Atkinson, R. *J. Phys. Chem. Ref. Data, Monograph 2* 1994.

(86) Lebeau, E. L.; Binstead, R. A.; Meyer, T. J. *J. Am. Chem. Soc.* **2001**, *123*, 10535 and references therein. (b) Mayer, J. M.; Hrovat, D. A.; Thomas, J. L.; Borden, W. T. *J. Am. Chem. Soc.* **2002**, *124*, 11142.
(87) Larsen N. W. *J. Mol. Structure* **1979**, *51*, 175.
(88) Portalone, G.; Schultz, G.; Domenicano, A.; Hargittai, I. *Chem. Phys. Lett.* **1992**, *197*, 482.
(89) Luzhkov, V. B.; Zyubin, A. S. *J. Mol. Struct. (THEOCHEM)* **1988**, *170*, 33.
(90) Chipman, D. M.; Liu, R.; Zhou, X.; Pulay, P. *J. Chem. Phys.* **1994**, *100*, 5023.
(91) Qin, Y.; Wheeler, R. *J. Chem. Phys.* **1995**, *102*, 1689.
(92) Olivella, S.; Solé, A.; García-Raso, A. *J. Phys. Chem.* **1995**, *99*, 10549.
(93) Liu, R.; Morokuma, K.; Mebel, A. M.; Liu, M. C. *J. Phys. Chem.* **1996**, *100*, 9314.
(94) Hammond, G. S. *J. Am. Chem. Soc.* **1955**, *77*, 334.
(95) Kreilick, R. W.; Weissman, S. I. *J. Am. Chem. Soc.* **1966**, *88*, 2645.
(96) Mahoney, L. R.; deRooge, M. A. *J. Am. Chem. Soc.* **1972**, *94*, 7002.
(97) Howard, J. A.; Furimsky, E. *Can. J. Chem.* **1973**, *51*, 3738.
(98) Mahoney, L. R.; deRooge, M. A. *J. Am. Chem. Soc.* **1975**, *97*, 4722.
(99) Ingold, K. U.; Burton, G. W.; Foster, D. O.; Zuker, M.; Hughes, L.; Lacelle, S.; Lusztyk, E.; Slaby, M. *FEBS Lett.* **1986**, *205*, 117.
(100) *JANAF Thermochemical Tables*, 3rd ed.; Chase, M. W., Jr., Davies, C. A., Downey, J. R., Frurip, D. J., McDonald, R. A., Syverud, A. N., Eds.; National Bureau of Standards: Washington, DC, 1985; Vol. 14.
(101) Truhlar, D. G.; Garrett, B. C. *J. Am. Chem. Soc.* **1989**, *111*, 1232.
(102) Kreevoy, M. M.; Truhlar, D. G. In *Investigation of Rates and Mechanisms of Reaction*, 4th ed.; Bernasconi, C. F., Ed.; Wiley: New York, 1986; Part I.
(103) Baulch, D. L.; Cobos, C. J.; Cox, R. A.; Esser, C.; Frank, P.; Just, Th.; Kerr, J. A.; Pilling, M. J.; Troe, J.; Walker, R. W.; Warnatz, J. *J. Phys. Chem. Ref. Data*, 1992; Vol. 81, no 3.
(104) Seinfeld, J. H.; Pandis, S. N. *Atmospheric Chemistry and Physics*; John Wiley: New York, 1998.
(105) Javanovic, S. V.; Simic, M. G. *J. Am. Chem. Soc.* **1986**, *108*, 5968.
(106) Cadete, J.; Delatour, Th.; Douki, Th.; Gasparutto, D.; Pauget, J.-P.; Ravanat, J.-L.; Sauvaigo, S. *Mutat. Res.* **1999**, *424*, 9.
(107) Goldstein, S.; Czapski, G. *Chem. Res. Toxicol.* **2000**, *13*, 736.
(108) Matuszak, Z.; Reszka, K. J.; Chignell, C. F. *Free Rad. Biol. Med.* **1997**, *23*, 367.
(109) Turjanski, A. G.; Rosenstein, R. E.; Estrin, D. A. *J. Med. Chem.* **1998**, *41*, 3684.
(110) Poeggeler, B.; Pappolla, M. A.; Hardeland, R.; Rassoulpour, A.; Hodgkins, P. S.; Guidetti, P.; Schwarcz, R. *Brain Res.* **1999**, *815*, 382.